

## CHAPTER 4

# PLASTIC-BASED SERS SUBSTRATE FOR THE DETECTION OF PESTICIDES IN WATER SAMPLES

---

In this chapter, polyethylene terephthalate (PET) plastic sheet has been used to fabricate flexible and transparent SERS substrates. AgNPs are drop-casted on the PET sheets to fabricate this SERS substrate. The reproducibility and enhancement of fabricated SERS substrates are characterized by detecting Raman active dye malachite green (MG). These SERS substrates are sensitive, cost-effective, flexible, and transparent which help to collect SERS signals in-situ from pesticide contaminated surfaces.

---

### 4.1 Introduction

The unique fingerprinting capability along with high sensitivity enabling SERS technique to emerge as one of the promising chemical and biomolecular detection platform in recent years [1]. Utilization of SERS-based techniques can be found in the fields like environmental monitoring, medical diagnosis, pharmaceutical research, food safety and forensic sciences. Pesticides have been extensively used in agriculture to enhance the crop yield by eliminating different insects, fungi, weeds and other pests. Presence of these pesticides eventually found in natural resources like water, fruits, vegetables and different packaged food products. Most of the synthetic pesticides are harmful to human health leading to various acute and chronic diseases [2, 3]. Therefore, detection of pesticides is critical for food safety management and environmental protection. Gas chromatography combined with mass spectrometry and liquid chromatography are commonly used for such purposes [4]. But, these instruments are very expensive, bulky, involves time-consuming sample preparation and detection process as well. Thus, there is a need for reliable, highly sensitive, selective and on-site pesticide detection methods. In that aspect, SERS has emerged as a promising platform for pesticide detection and identification due to its high sensitivity, selectivity, and fast and cost-effective technique [5–8]. There is a large number of literature containing innovative SERS

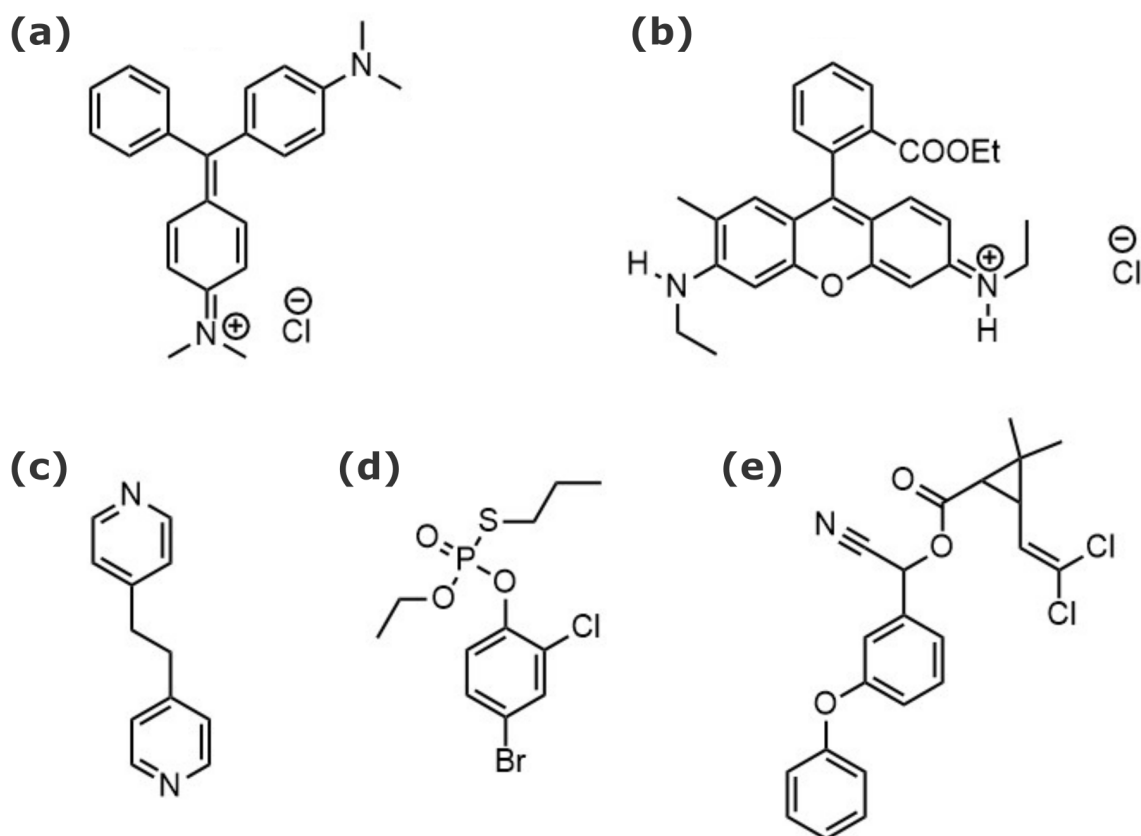


Figure 4.1: Chemical structure of (a) malachite green, (b) rhodamine 6G, (c) 1,2-bis(4-pyridyl)ethylene, (d) profenofos and (e) cypermethrin.

substrates for sensitive and accurate identification of different class of pesticides are available. However, more research is required on reliable SERS techniques for fast and in-situ detection and identification of pesticides.

Flexible and transparent plastic sheets have the potential to be used as the base of SERS substrates where plasmonic nanoparticles can be immobilized. In the present thesis work, AgNPs drop-casted on PET sheets have been used as low-cost and sensitive SERS substrates. The reproducibility and enhancement factor (EF) of the fabricated SERS platform have been initially characterized with the Raman active sample MG. Upon noticing the reliable performance on the standard Raman analyte, its usability has been demonstrated for detection of two pesticide samples. The proposed SERS substrate is flexible and transparent which could help to collect SERS signals in-situ from pesticide-contaminated surfaces.

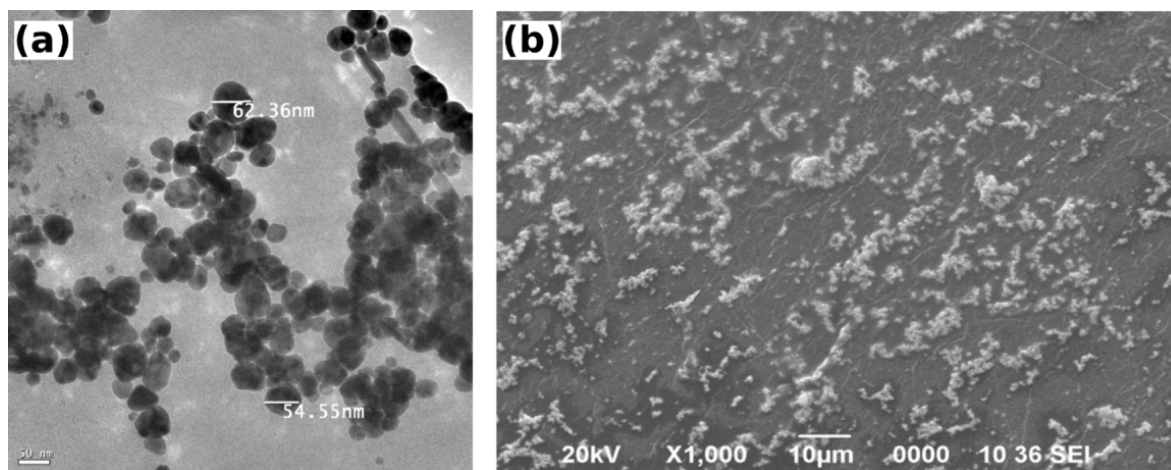


Figure 4.2: (a) TEM image of the synthesized AgNPs. (b) SEM image of the surface of the plastic-base SERS substrate.

## 4.2 Materials and methods

### 4.2.1 Materials

Trisodium citrate dihydrate ( $C_6H_5Na_3O_7 \cdot 2H_2O$ ) and silver nitrate ( $AgNO_3$ ) were purchased from Merck, India. Raman active molecule malachite green ( $C_{23}H_{25}ClN_2$ ) was procured from Alpha Aesar, India. PET plastic sheet was purchased from a local stationary shop. Pesticide Googly (profenophos 40% + cypermethrin 4% EC) from Anu Products Limited was purchased from local supplier. All chemicals were utilized as supplied without additional processing and deionized (DI) water was employed to prepare all experimental samples.

### 4.2.2 SERS substrate fabrication process

Colloidal AgNPs required for the proposed SERS substrate have been synthesized following the standard Lee-Meisel method [9]. In this technique, trisodium citrate (TSC) has been used as a reducing and stabilizing agent. 1 mM of  $AgNO_3$  and 1 wt% of TSC were prepared in DI water. 100 mL of  $AgNO_3$  solution was added in a 250 mL conical flask and was heated for 15 minutes till the solution boils. 4 mL of TSC was added rapidly to the boiling  $AgNO_3$  solution. The mixture was then stirred vigorously for 1 hour until the colour of the solution turns yellow. Figure 4.2(a) represents the TEM image of the synthesized AgNPs. From the figure, the dimension of the AgNPs have been found to be around 50-60 nm.

To fabricate the SERS substrates, commercially available PET plastic sheet has been considered. This sheet was cut into several small pieces each of dimension 10 mm  $\times$  10 mm, and 10  $\mu$ L volume of the synthesized AgNP solution was drop-casted on each of the plastic substrates. These AgNP-treated plastic pieces were then placed in a

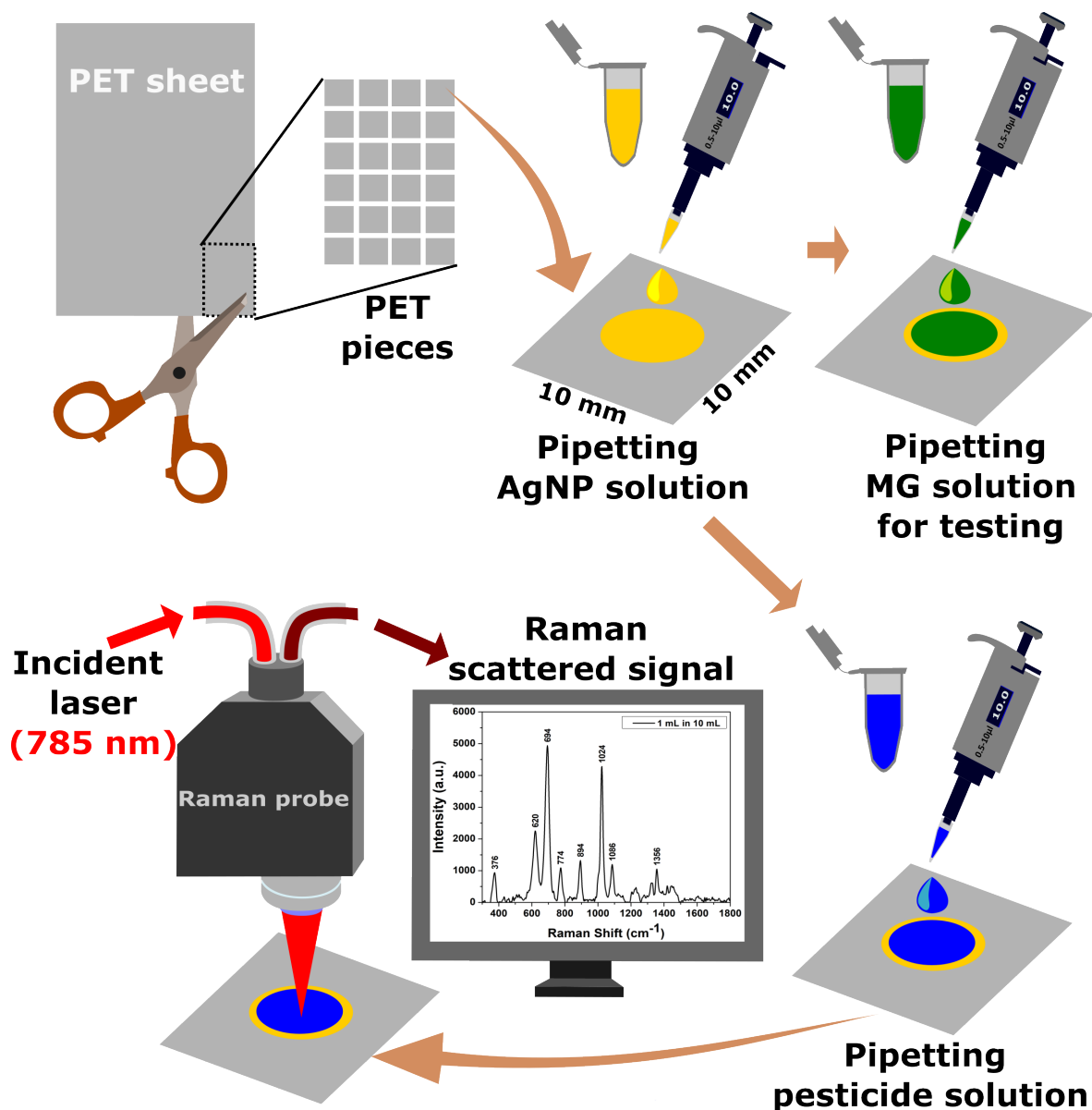


Figure 4.3: Schematic representation of the fabrication process of the AgNP decorated PET-based SERS substrate and the pictorial depiction of the Raman signal collection.

vacuum desiccator for 2 hour for drying before using these as a SERS substrate. Figure 4.2(b) displays the SEM image of the fabricated SERS substrate. The AgNPs have formed small clusters which are almost uniformly distribute over the PET substrate.

#### 4.2.3 COMSOL simulation for the fabricated SERS substrates

Simulation study has been carried out to understand the distribution of the electric field scattered by the AgNPs distributed over the plastic substrate. The dimension and distribution of the AgNPs are taken from the TEM and SEM images in the figure 4.2. Here, two AgNPs of diameter 50 nm each have been considered which are separated by a distance 5 nm are placed on the PET substrate, and a laser light of wavelength

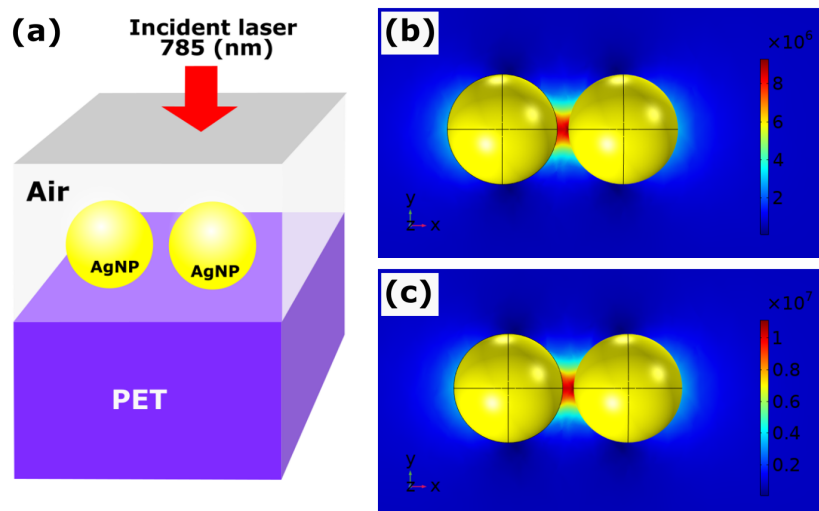


Figure 4.4: (a) Schematic representation of laser light incident on 2 AgNPs in air placed on a PET base. Scattered electric field distribution when 785 nm laser is incident on the nanoparticles (b) from air medium and (c) through the plastic substrate.

785 nm is allowed to incident on the AgNPs. The intensity of the incident electric field is kept fixed at the value  $1 \times 10^9 \text{ Wm}^{-2}$  and power at 0.25 mW. In the first case, the laser light is allowed to incident on the AgNPs from air medium as shown in the figure 4.4(a). Figure 4.4(b) represents the localized electric field for this condition. From figure 4.4(b), the maximum value of the scattered electric field is found to be  $9.28 \times 10^6 \text{ Vm}^{-1}$ . In another case, the incident light is allowed to pass through the PET layer and then incident on the AgNPs. Figure 4.4(c) represents the scattered electric field distribution for two AgNPs in this case, and the maximum value of the coupled field is calculated to be  $1.11 \times 10^7 \text{ Vm}^{-1}$ . Comparing figure 4.4(b) and 4.4(c), a 19.6% increase in the scattered electric field has been observed when the laser is passing through the PET layer and then incident on the nanoparticles.

## 4.3 Results and discussions

### 4.3.1 SERS performance of the fabricated substrate

Performance of the fabricated SERS substrates has been evaluated using a Raman spectrometer equipped with a 785 nm diode laser. Figure 4.5(a) depicts the Raman spectrum of the PET sheet. The characteristic peaks at  $1186 \text{ cm}^{-1}$ ,  $1416 \text{ cm}^{-1}$ ,  $1616 \text{ cm}^{-1}$  and  $1728 \text{ cm}^{-1}$  are assigned to the ring in plane C–H bond and C–C stretch, CCH bending and OCH bending, ring breathing mode and C=O stretching vibration, respectively [10]. Next, Raman spectra have been collected from the sensing region of the fabricated plastic SERS substrate. In addition to normal Raman signal collection, the SERS substrate has been flipped carefully and Raman spectra have been collected

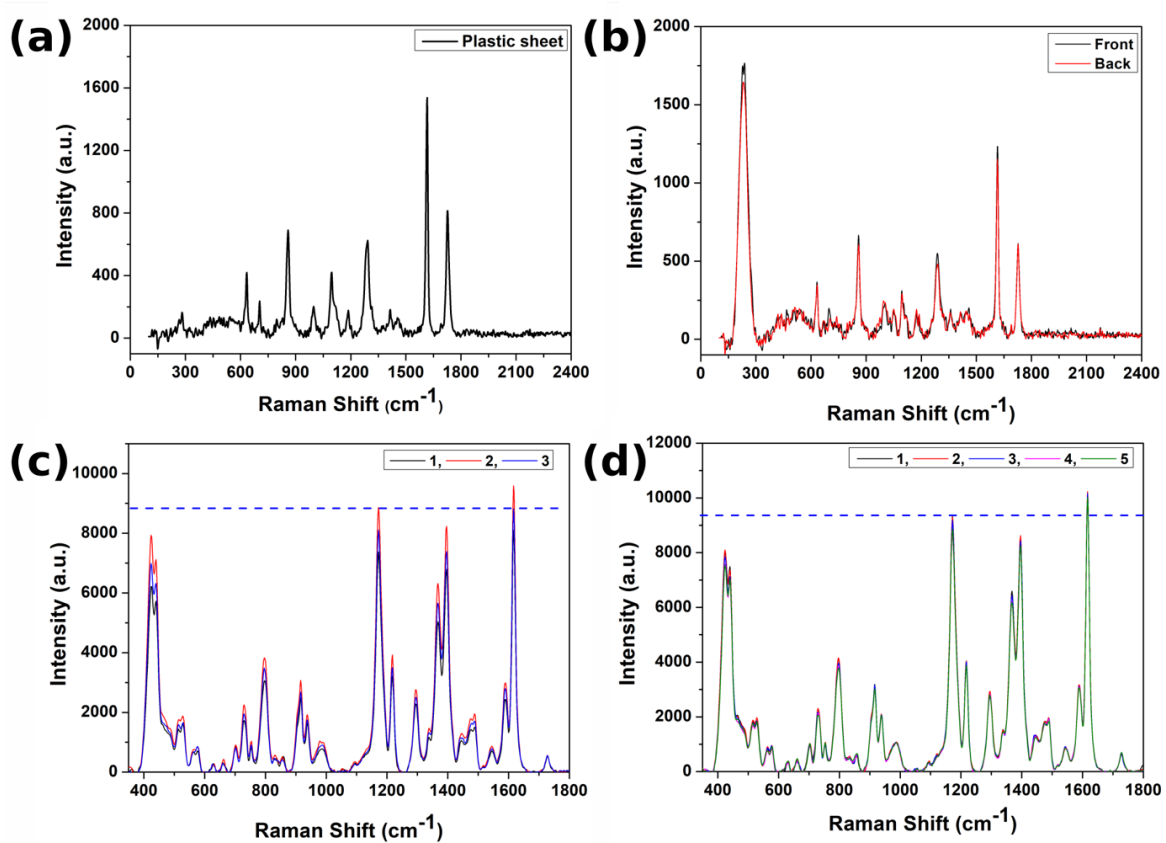


Figure 4.5: (a) Raman spectrum of the PET sheet. (b) Raman spectra of the plastic SERS substrate when collected from the front and rear of the SERS sensitive region. SERS spectra of 20  $\mu\text{M}$  MG collected from the (c) front and through the (d) rear side of the transparent SERS substrates.

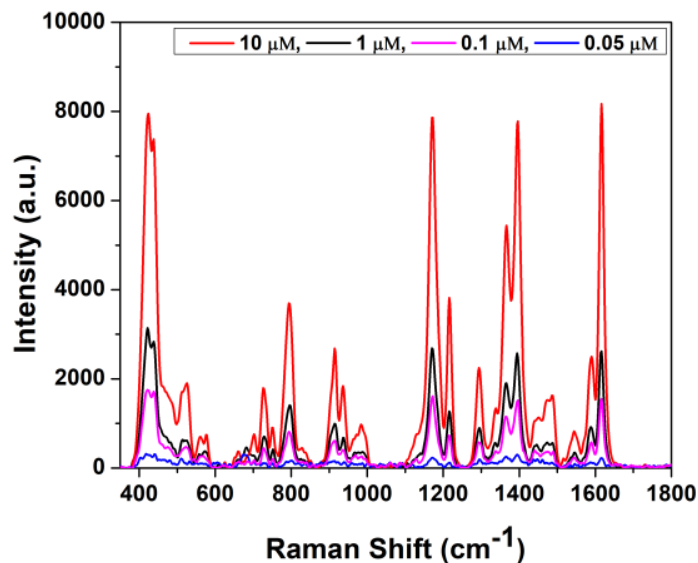


Figure 4.6: Variation of Raman signal intensity with the concentration of MG from 10  $\mu\text{M}$  to 50 nM collected from PET-based SERS substrate.

from the rear side of the SERS substrate. Both the Raman signals are represented in figure 4.5(b). A solution of 20  $\mu\text{M}$  MG was prepared and three drops of 10  $\mu\text{L}$  volume of this solution have been pipetted on the sensing region of three fabricated SERS substrates. After 1 hour of drying in vacuum desiccator, Raman spectra were collected from 3 different SERS substrates (average spectra are shown in figure 4.5(c)) on the front surface of the SERS substrates. The characteristic peaks of MG at 796  $\text{cm}^{-1}$ , 1172  $\text{cm}^{-1}$ , 1216  $\text{cm}^{-1}$ , 1390  $\text{cm}^{-1}$ , and 1614  $\text{cm}^{-1}$  are attributed to ring C-H out-of-plane bending, ring C-H in-plane vibration, C-H rocking, N-phenyl stretching and ring C-C in-plane stretching vibrations, respectively [11]. After that, the MG treated SERS substrates were flipped and Raman spectra were collected from the rear side of the proposed SERS platform. Figure 4.5(d) shows the Raman signal collected from 5 different points of a SERS substrate. Average SERS signal intensity for the peak 1172  $\text{cm}^{-1}$  in the figure 4.5(c) and 4.5(d) are calculated to be 8110 and 9090, respectively. This represent a total 12% increase in the Raman signal intensity of MG when the signal is collected from the rear side of the substrate compared to the normal SERS signal collection. From figure 4.5(a) and 4.5(b), it has been observed that ultra-low concentration of MG could not be detected utilizing PET-based SERS substrates as the background signal is too high.

Figure 4.6 represents the SERS spectral intensity variation for 4 different concentrations of MG collected using the fabricated PET-based SERS substrate. The average enhancement factor ( $EF_{avg}$ ) of the developed SERS substrate has been estimated using the following equation as discussed in the section 1.3.3:

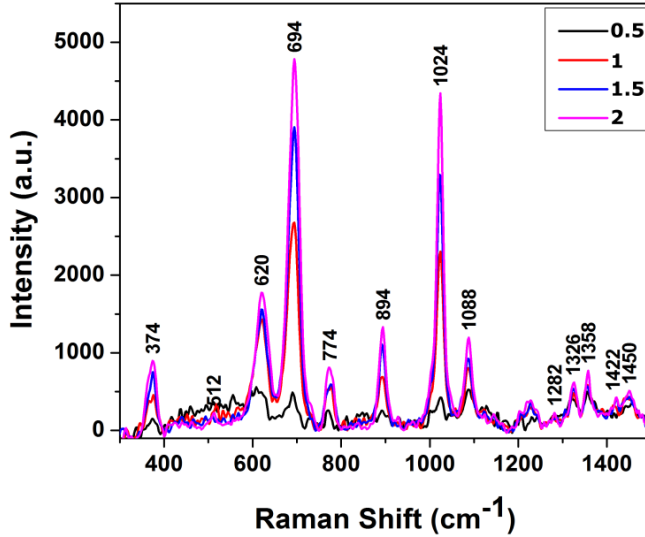


Figure 4.7: Variation of Raman signal intensity with the concentration of pesticide sample from 2  $\mu\text{L}/\text{mL}$  to 0.5  $\mu\text{L}/\text{mL}$  collected from PET-based SERS substrate.

$$EF_{avg} = \frac{\frac{I_{SERS}}{N_{SERS}}}{\frac{I_{Raman}}{N_{Raman}}}, \quad (4.1)$$

where,  $I_{SERS}$  and  $I_{Raman}$  represent SERS and normal Raman scattering intensities, respectively.  $N_{SERS}$  and  $N_{Raman}$  represents the number of analyte molecules probed for SERS and normal Raman scattering measurements, respectively. First, 10  $\mu\text{L}$  of MG of concentration 10 mM has been pipetted on a bare substrate and dried in a vacuum desiccator for 1 hour. Raman spectra of MG from different points of the plane substrate were recorded. From figure 4.5, MG solution of minimum concentration, 0.05  $\mu\text{M}$  has been detected using the PET-based SERS substrate. Next, 10  $\mu\text{L}$  MG of concentration 0.05  $\mu\text{M}$  has been pipetted on the sensing region of the proposed SERS substrate. Upon drying, Raman spectra were collected and average Raman signal intensity for the peak at 1172  $\text{cm}^{-1}$  was estimated. The average enhancement factor,  $EF_{avg}$  has been calculated to be  $3 \times 10^5$ .

### 4.3.2 SERS spectra of pesticide sample

As suggested by the manufacturer, insecticide Googly of volume 200 mL has been mixed with 200-400 L of water and sprayed in the agriculture field by the farmers. In the present work, 2  $\mu\text{L}$  of the pesticide sample has been mixed with 1 mL of DI water. From this mixture, several lower concentrated samples have been prepared by serial dilution. 10 L of volumes of the pesticide solutions were pipetted on the sensing region of the PET-based SERS substrates. Variation of Raman signal intensity with the concentration of pesticide sample from 2  $\mu\text{L}/\text{mL}$  to 0.5  $\mu\text{L}/\text{mL}$  has been represented



---

in the figure 4.7. Chemical structures of the two pesticide samples have been shown in the figure 4.1(d-e). In the figure 4.7, the characteristic Raman peaks of the pesticide solution have been found at  $374\text{ cm}^{-1}$ ,  $620\text{ cm}^{-1}$ ,  $694\text{ cm}^{-1}$ ,  $774\text{ cm}^{-1}$ ,  $894\text{ cm}^{-1}$ ,  $1024\text{ cm}^{-1}$ ,  $1088\text{ cm}^{-1}$ ,  $1326\text{ cm}^{-1}$  and  $1356\text{ cm}^{-1}$ . The sharp peak at  $1024\text{ cm}^{-1}$  is arising due to the benzene ring breathing mode. The peak at  $694\text{ cm}^{-1}$  and  $774\text{ cm}^{-1}$  are attributed to bending vibration of P-S and stretching vibration of P-O of profenofos molecule, respectively [12]. As the concentration of cypermethrin in the solution is very small, its characteristic peak (ring breathing mode at  $1003\text{ cm}^{-1}$ ) are not distinguishable in the figure 4.7 [13, 14].

## 4.4 Summary

In this chapter, flexible and transparent SERS substrates are fabricated by drop-casting AgNPs over commercially available plastic sheets. Significant Raman signal enhancement has been observed when the Raman signals are collected from the backside of the MG treated transparent SERS substrates. Fabricated SERS substrates are applied in the sensitive detection and identification of insecticides in water.

## Bibliography

- [1] Langer, J., Jimenez de Aberasturi, D., Aizpurua, J., Alvarez-Puebla, R. A., Augu e, B., Baumberg, J. J., Bazan, G. C., Bell, S. E., Boisen, A., Brolo, A. G., et al. Present and future of surface-enhanced raman scattering. *ACS nano*, 14(1): 28–117, 2019.
- [2] Kim, K.-H., Kabir, E., and Jahan, S. A. Exposure to pesticides and the associated human health effects. *Science of the total environment*, 575:525–535, 2017.
- [3] Pinto, B. G. S., Soares, T. K. M., Linhares, M. A., and Ghisi, N. C. Occupational exposure to pesticides: Genetic danger to farmworkers and manufacturing workers—a meta-analytical review. *Science of the Total Environment*, 748:141382, 2020.
- [4] Alder, L., Greulich, K., Kempe, G., and Vieth, B. Residue analysis of 500 high priority pesticides: better by gc–ms or lc–ms/ms? *Mass spectrometry reviews*, 25 (6):838–865, 2006.
- [5] Mikac, L., Kova evi c, E., Uki c,  . S., Rai c, M., Jurkin, T., Mari c, I., Goti c, M., and Ivanda, M. Detection of multi-class pesticide residues with surface-enhanced raman spectroscopy. *Spectrochimica Acta Part A: Molecular and Biomolecular Spectroscopy*, 252:119478, 2021.

- 
- [6] Pang, S., Yang, T., and He, L. Review of surface enhanced raman spectroscopic (sers) detection of synthetic chemical pesticides. *TrAC Trends in Analytical Chemistry*, 85:73–82, 2016.
- [7] Jiang, Y., Sun, D.-W., Pu, H., and Wei, Q. Surface enhanced raman spectroscopy (sers): A novel reliable technique for rapid detection of common harmful chemical residues. *Trends in food science & technology*, 75:10–22, 2018.
- [8] Bernat, A., Samiwala, M., Albo, J., Jiang, X., and Rao, Q. Challenges in sers-based pesticide detection and plausible solutions. *Journal of agricultural and food chemistry*, 67(45):12341–12347, 2019.
- [9] Deshpande, J., Chakrabarty, S., and Kulkarni, A. Heterogeneous nucleation in citrate synthesis of agnps: Effect of mixing and solvation dynamics. *Chemical Engineering Journal*, 421:127753, 2021.
- [10] Rebollar, E., Pérez, S., Hernández, M., Domingo, C., Martín, M., Ezquerra, T. A., García-Ruiz, J. P., and Castillejo, M. Physicochemical modifications accompanying uv laser induced surface structures on poly (ethylene terephthalate) and their effect on adhesion of mesenchymal cells. *Physical Chemistry Chemical Physics*, 16(33):17551–17559, 2014.
- [11] Kumar, P., Khosla, R., Soni, M., Deva, D., and Sharma, S. K. A highly sensitive, flexible sers sensor for malachite green detection based on ag decorated microstructured pdms substrate fabricated from taro leaf as template. *Sensors and Actuators B: Chemical*, 246:477–486, 2017.
- [12] Lu, Y., Tan, Y., Xiao, Y., Li, Z., Sheng, E., and Dai, Z. A silver@ gold nanoparticle tetrahedron biosensor for multiple pesticides detection based on surface-enhanced raman scattering. *Talanta*, 234:122585, 2021.
- [13] Sivashanmugan, K., Lee, H., Syu, C.-H., Liu, B. H.-C., and Liao, J.-D. Nanoplasmonic au/ag/au nanorod arrays as sers-active substrate for the detection of pesticides residue. *Journal of the Taiwan Institute of Chemical Engineers*, 75:287–291, 2017.
- [14] Sitjar, J., Hou, Y.-C., Liao, J.-D., Lee, H., Xu, H.-Z., Fu, W.-E., and Chen, G. D. Surface imprinted layer of cypermethrin upon au nanoparticle as a specific and selective coating for the detection of template pesticide molecules. *Coatings*, 10(8):751, 2020.